(Received 8 April 2026, Accepted 26 May 2026, Scheduled 12 June 2026)

Safety Constrained Sparse Radiation Therapy via Efficient Optimization Approach for Biomedical Phased Array Applications

Ahmed J. Abdulqader[1,*], Huda A. Al-Tayyar[2], and Yessar E. Mohammed Ali[3]

[1] College of Electronics Engineering, Ninevah University, Mosul-41002, Iraq
[2] College of Engineering, Department of Communications and Intelligent Digital Systems Engineering, University of Mosul Mosul-41002, Iraq
[3] College of Engineering, Department of Computer and Communications Engineering, Nawroz University, Duhok-42001, Iraq

ABSTRACT: The development of interventional radiotherapy techniques has become one of the most important concerns for antenna designers worldwide. In this study, an efficient optimization approach based on a hybrid algorithm that exploits the quantitative concept and the theory of reinforcement convexity, called the quantitative-convex approach (QCA), is presented to produce a high-performance electromagnetic radiation pattern. The novelty of this study lies in shaping patterns that mimic the shape of the targeted human organ in radiotherapy by steering a flat main beam from a square antenna array, along with optimal control of the sidelobe level. The proposed approach works by identifying the diseased organ captured from medical imaging, converting it into a binary image (black and white colors), and then feeding it into the antenna system to form a radiation pattern that accurately mimics the diseased organ. To reduce the systemic and computational complexity of the therapeutic antenna system, a sparsity technique was added to the hybrid algorithm. The computer simulation results showed high efficiency in generating robust patterns with sharp boundary profiles, such as those used for isolating diseased and undiseased tissues and measuring the tissue-specific absorption rate (TSAR), making it suitable for use in radiotherapy.

1. INTRODUCTION

For many years, the exploitation of microwave capabilities in medical applications has been studied for diagnostic, therapeutic, and developmental purposes [1, 2]. In recent years, this topic has attracted increasing attention from many researchers owing to the significant and remarkable development of phased array technology. The enhanced capabilities of radiation systems in such arrays provide many uses that can be exploited tremendously in the field of healthcare and take full advantage of their radiation capabilities, especially because they are safe for humans and noninvasive procedures. Despite the aforementioned advantages, the design of phased arrays for medical purposes faces difficult challenges, both practically and analytically, which necessitate a complete understanding of the fundamentals of array slot design.

There are many prominent medical applications based on radiation therapy, including microwave-based thermal therapy for cancer treatment [3, 4]. This application works on the principle of selective heating of cancerous tissues based on their energy loss. Thermal radiation therapy is used to combat malignant tumors or increase the effectiveness of specific treatments (radiation therapy and chemotherapy), which increases the likelihood of patient recovery. The challenge in these cases lies in allocating a sufficient number of radiating elements in the array and feeding them efficiently, thus providing sufficient degrees of freedom to form a therapeutic or diagnostic beam. It is important to consider that the complexity of the radiation system must be reduced, thus simplifying its repair. In this form, it is necessary to transfer the radiation energy correctly to the treatment area without any radiation errors that can cause damage to healthy biological tissues [5, 6].

The use of microwave-based radiation therapy techniques depends on the electrical properties of the targeted human tissues in terms of their physiological condition and tissue type. This requires the operation of a large number of radiating elements and the combination of their electromagnetic signals to form a suitable therapeutic beam pattern. This is very important for the reliability of the results of diagnosis and treatment by increasing the amount of information obtained, which positively affects the translation of the correct diagnosis of the disease and its treatment. This means that accurate imaging of the human organ to be treated with radiation is one of the most prominent challenges faced by designers because of the reliance on this imaging in radiation therapy. Breast cancer imaging has been a common example in this field over the past two decades [7]. In all medical applications, whether diagnostic or therapeutic, the design of phase arrays in terms of the number, location, type, and polarization of radiating elements is an important engineering consideration that must be taken into account. The most important of these parameters is to reduce the number of ra-

* Corresponding author: Ahmed Jameel Abdulqader (ahmed.abdulqader@uoninevah.edu.iq).

diating antennas as much as possible, but not at the expense of the radiation system's performance in building the desired therapeutic pattern, which greatly contributes to reducing the treatment time and the necessary costs.

Also, one of the difficult challenges facing the design of phased antenna arrays in medical applications is that the therapeutic target area may be located in the near field of the array radiation, and the two areas are usually immersed in a matching medium, resulting in a loss for treatment. Also, the therapeutically targeted area may have a three-dimensional band, which has heterogeneous electrical properties, causing high radiation loss, and this varies from tissue to tissue depending on the patient. To overcome this problem, the shape of the phased array aperture depends on the anatomy of the target area before radiotherapy to achieve complete conjugation and penetration. Choosing the right type of array topology standard to resolve the aforementioned differences is a key priority when designing a radiation antenna system, especially concerning the spatial distribution of the radiating elements on a grid of points spaced at half the wavelength. Then, choosing the right topology provides the optimal choice of antenna positions, thus enabling fruitful exploitation of degrees of freedom and avoiding the generation of high sidelobes or undesirable grating lobes that could affect healthy tissues during treatment. Also, this provides a direct result of a homogeneous Fourier transform relationship between the radiating element excitations and the array factor in the far field [8]. However, in medical applications, the radiation array system is usually close to the target areas to be treated. Therefore, designing antenna arrays with elements spaced at a distance of $\lambda/2$ may involve a large number of radiating elements, causing an increase in the complexity and cost of the system. There is also another issue that affects the number of radiating elements, which is the small size of the human body organs that need to be treated with radiation. Therefore, reducing the size of antennas allows for a suitable increase in the number of elements, especially in the treatment of small tumors, thanks to their small dimensions. In practice, several types of antennas have been proposed for building the desired therapeutic radiation array, including those mentioned in [9] and [10]. In summary, the main challenge in building a therapeutic radiation array is to form a precise therapeutic beam pattern that features highly flexible electromagnetic performance to direct the beam to a specific tissue area and avoid damaging other healthy tissue areas. This can be achieved by forming a radiation pattern with a main beam resembling the diseased tissue area, while greatly reducing the proportion of sidelobes and also generating a null steering to avoid nearby tissue damage. These features require an efficient and fast algorithm that delivers the appropriate stimuli to shape the desired therapeutic pattern. It is possible to use biological or mathematical algorithms, such as genetic algorithm [11], particle swarm optimization (PSO) [12], convex optimization [13], and compressed sensing [14].

In this study, an integrated and efficient approach based on an optimization system for synthesizing antenna array radiation patterns for medical purposes was presented, relying on sharing the computational quantum concept without the need for quantum equipment, in coordination with the mathematical convex algorithm. The proposed method offers a radiation system to generate flat patterns resembling a diseased human organ or part of it by utilizing a medical imaging system. Medical imaging of the targeted organ is performed to extract the diseased area after converting it into a binary image consisting of black and white pixels using a digital image processing technique to isolate the diseased (white) and non-diseased (black) tissues. The sparsity technique was incorporated into the hybrid optimization system to reduce the number of active elements involved in the synthesis of the required radiation patterns, thereby reducing the systemic and computational complexity and cost. All calculations performed in this study were obtained using MATLAB.

2. MATHEMATICAL MODEL FOR RADIATION THERAPY

To build a suitable radiation system for therapeutic purposes, an efficient device capable of generating an electromagnetic beam pattern according to precise therapeutic requirements must be designed. From a dynamic perspective, the designed radiographic device must be capable of reconfiguring the radiographic pattern to cope with changes in the disease area from one patient to another. In practice, in radiating antenna systems, beam pattern reconfiguration can only be achieved by exploiting the excitation of the elements in the array. Therefore, a suitable antenna array must be selected based on the available information about the target disease area and the clarity of the diseased tissues within it, providing a clear view for constructing the therapeutic beam pattern. The use of a two-dimensional array for this purpose is considered a successful radiation system. A set of symbols was used in the structure of the mathematical model, which can be illustrated in Table 1.

TABLE 1. The definitions of symbols.

Symbol	Meaning
g	Aperture grid
E_{nm}	Complex feeding
I	Morphological electromagnetic distribution
β_{nm}	The probability of excitation of a phase
ξ	The phase optimization learning rate
τ	a small value for math purposes
α_1 and α_2	Parameters that determine the percentage of sparsing
γ	$[10^{-3}, 10^{-1}]$
ψ	$[10^{-4}, 10^{-2}]$
σ	Electrical conductivity
ρ	Mass density
T_{TSAR}	Hermitian matrix
Υ	Unity identical matrix

Let us consider an antenna array consisting of $N \times M$ elements distributed in a square grid and arranged with spacing equal to $\lambda/2$ between any two consecutive elements on the x-y

axes, such that the components of this grid are:

$$g = [x_n, y_m]_{n\times m=1\times 1}^{N\times M}, \text{ where}$$
$$x_n = d_x\left(n - \frac{N+1}{2}\right) \quad (1)$$
$$y_m = d_y\left(m - \frac{M+1}{2}\right)$$

where g represents the aperture grid in which the antenna elements are arranged, and $d_x = d_y$ is the equal distances between the elements on both axes. The array factor ($\mathbb{F}$) for this aperture can be expressed as follows [8]:

$$\mathbb{F}(\theta,\phi) = \sum_{n=1}^{N}\sum_{m=1}^{M} E_{nm}\exp\left(j\frac{2\pi}{\lambda}(x_n u_o + y_m v_o)\right) \quad (2)$$

where $E_{nm} = |E_{nm}|\, e^{j\angle E_{nm}}$ is the complex feeding that excites each element in the array, and (u_o, v_o) is the main beam orientation axis of the array in (u, v) coordinates.

$$u_o = \sin\theta_o\cos\phi_o \quad v_o = \sin\theta_o\sin\phi_o \quad (3)$$

Eq. (2) can be simplified to:

$$\mathbb{F}(\theta,\phi) = E_{nm}P \quad (4)$$

where $P = \exp(j\frac{2\pi}{\lambda}(x_n u_o + y_m v_o))$. To build a highly efficient radiation therapy system, several challenges and obstacles must be overcome in the antenna system. The greatest challenge lies in forming a specific radiation pattern, which means that the traditional array can synthesize regular flat patterns, such as a square and a rectangle. Therefore, the beam pattern of such arrays does not meet the requirements of medical applications in radiation therapy of targeted tissues, which may negatively affect healthy tissues. Synthesizing arrays with applied radiation in medical treatments, such as heat-killing malignant tumors by projecting electromagnetic radiation onto them after determining the shape of the tumor (i.e., the damaged tissues), is very important to provide a suitable radiation area to maximize the durability of radiation therapy and reduce damage to healthy tissues. To do this, in this study, the results of images extracted from medical imaging devices such as MRI or CT are relied upon, and the distribution of the electromagnetic field is extracted from them to identify diseased and non-diseased tissues. The medical image is then processed using an image processing technique into a two-color image, presented as a white and black mask. White represents diseased tissue, and black represents healthy tissue. Mathematically, the covering mask is represented as $MC(\theta,\phi) \in [0,1]$. The mask determines the shape, size, and dimensions of the radiation target area at maximum power. This situation provides the advantage of avoiding healthy tissues (the non-target area) from radiation, which enables the system's algorithm to control the radiation power directed at the patient with high accuracy. This means that the target area has a high specific absorption rate. By combining this mask with the array factor of the antenna system, we obtain:

$$|\mathbb{F}(\theta,\phi)| = E_{nm}P\cdot MC(\theta,\phi) \quad (5)$$

To confirm that the generated beam pattern matches the enhanced black and white medical image, a conditional parameter called shape accuracy parameter (SAP) was added to the algorithm and is represented by:

$$\text{SAP} = \||\mathbb{F}(\theta,\phi)| - I\|_2^2 \quad (6)$$

I represents the morphological electromagnetic distribution dependent on the amplitude-phase excitation of radiating elements using a convex algorithm for the target tissue area extracted from the medical image. This condition reconstructs the therapeutic beam pattern with high precision, ensuring that damage to other tissues is avoided. To increase the accuracy of the radiographically formed pattern so that it perfectly matches the targeted diseased region, the phase excitation alone is synthesized using a quantum concept without adding a new objective function. This is achieved by exploiting the degrees of freedom of the phases that were partially neglected in the convexity improvement stage of Eq. (6). The proposal of the concept of quantum computing here does not mean the use of quantum devices in the physical sense (i.e., it does not mean the use of quantum implementations with quantum devices), but rather the application of the concept of the quantum state to improve the feeding phases of the elements separately from the amplitudes by representing the mathematical state based on probability and angular rotation for each assigned phase. Therefore, the initial phases can be defined as follows:

$$\angle E_{nm} \in \left\{0, \frac{\pi}{2}, \pi, \frac{3\pi}{2}\right\} \quad (7)$$

Then, the phase excitation of each radiating element is denoted by a quantum state as follows:

$$|q_{nm}\rangle = [\cos\beta_{nm} \;\; \sin\beta_{nm}], \quad \beta_{nm} \in [0, 2\pi] \quad (8)$$

where β_{nm} represents the probability of excitation of a phase for each radiating element. Consequently, it enables the simultaneous identification of multiple phase hypotheses for a single stage in the optimization process, which is crucial for the diversity of searches for optimal results in deterministic approximations. Therefore, these phases can be continuously updated by performing the following iterations:

$$\beta_{nm}^{(k+1)} = \beta_{nm}^{(k)} + \xi\frac{\partial SAP}{\partial\angle E_{nm}} \quad (9)$$

where ξ is the phase optimization learning rate. Eq. (9) provides a phase simulation update mechanism in the quantum state, thus enabling the flexible exploration of phase excitability discretely. To date, the optimization process has relied on synthesizing all radiating elements separately. After achieving the desired convergence through quantitative phase updates for each element, all phases were prepared to participate in the subsequent master optimization process. So:

$$\angle E_{nm} = \arg\min_{\angle E_{nm}\in\left\{0,\frac{\pi}{2},\pi,\frac{3\pi}{2}\right\}} |\angle E_{nm}^{*} - \arg(|q_{nm}\rangle\rangle|$$
$$\text{where } \angle E_{nm}^{*} = \left\{0, \frac{\pi}{2}, \pi, \frac{3\pi}{2}\right\}^{*}, \quad nm \in \text{active set} \quad (10)$$

The final phases resulting from the quantum calculations are shared through the following model:

$$E_{nm}^{final} = |E_{nm}|\, e^{j\angle E_{nm}^{*}} \tag{11}$$

To reduce the complexity of the antenna system (i.e., reduce the number of radiating antennas), the sparse approach is incorporated into the main optimization process by using the zero-norm excitation (i.e., $\|E_{nm}\|_0$) principle. Consequently, the objective function Eq. (6) can be expressed as follows:

$$\text{SAP}_f = \sum_{s=1}^{S} \log(|E_{nm}| + \tau) \tag{12}$$

where τ is a small value, and s represents the number of sparse elements (active elements). From the perspective of synthetic sparsity optimization, this function adds an irregular contraction effect to the elements of the array through the log function, which imposes strict constraints on the elements that make a weak contribution to the synthesis process. Therefore, elements with weak contributions are reduced to zero (inactive state), whereas elements with effective contributions remain unchanged (active state). This approach allows the algorithm to automatically select effective elements quickly without incurring additional parameter costs. Moreover, the use of the sparse technique is suitable for radiation therapy applications because it reduces the number of active elements in the array owing to the generation of irregular spaces between the active elements, which reduces the leakage of unintended radiation into healthy tissues. Next, to regulate the flow of power excitation to the radiating elements, excitation norm 2 is entered into the target function as follows:

$$\text{SAP}_f = \|E_{nm}\|_2^2 \tag{13}$$

To prepare an objective function with computationally efficient and globally optimal convergence properties that provide convexity for all optimization constraints, a convex optimization function that incorporates all optimization requirements in terms of radiation therapy shape fidelity, sparsity constraints for the desired sparse, and energy flow control for the aperture elements was prepared as follows:

$$\begin{aligned} &\underbrace{\min_{E_{nm}} \| |\mathbb{F}(\theta,\phi)| - I \|_2^2}_{Radiation\ Therapy\ Shape\ Fidelity} \\ &+ \underbrace{\alpha_1 \sum_{s=1}^{S} \log(|E_{nm}| + \tau)}_{Sparsity\ Constraint} \\ &+ \underbrace{\alpha_2 \|E_{nm}\|_2^2}_{Power\ Excitation\ Control} \end{aligned} \tag{14}$$

α_1 and α_2 are parameters that determine the percentage of sparsing added to the array and the percentage of the total power input to the array, respectively. These parameters allow for a precise dynamic balance between forming an accurate medical beam pattern and minimizing radiating elements as much as possible, while providing the necessary safety standards for the patient. These two parameters are expressed as follows:

$$\begin{aligned} &\alpha_1 = \gamma.\max(\left|E_{nm}^{(k)}\right|), \ \text{where}\, \gamma \in \left[10^{-3}, 10^{-1}\right] \\ &\alpha_2 = \psi \cdot trace(P^H \cdot A), \ \ \psi \in \left[10^{-4}, 10^{-2}\right] \end{aligned} \tag{15}$$

where A is the array sensing matrix. Through several optimization experiments, it was found that choosing appropriate values for γ and ψ within the knowledge ranges in Eq. (15), as choosing inappropriate values outside the specified range, leads to excessive confusion in the therapeutic pattern or poor administrative organization of elements, which may produce unjustified solutions.

3. PATIENT MEDICAL SAFETY PROCEDURES

One of the considerations regarding medical safety procedures for patients that must be taken into account is the biological protection of organs when medical radiation is applied to the human body. The parameter responsible for verifying and detecting this safety is the TSAR, which expresses the rate of absorption of electromagnetic radiation by body tissues in targeted and non-targeted areas, as illustrated in the following model:

$$\text{TSAR} = \frac{\sigma\, |\mathbb{F}(\theta,\phi)|^2}{2\rho} \tag{16}$$

where σ represents the electrical conductivity, which is used to measure the flow of electrical energy reaching the tissues and depends on several factors, including the type of tissue concerned and the frequency of the applied light. ρ is the mass density of the target tissue. Regularly measuring these parameters provides the necessary protection for the patient, because neglecting them leads to damage to healthy tissues if the levels of TSAR are raised to a high degree of heating as a result of strong radiation. Therefore, it is important to incorporate this parameter into the radiation system design process. Mathematically, the TSAR-constraint imposed in the medical radiation synthesis process by the array system in the form of a quadratic vector ensures anatomical conformity to the required region and is expressed as follows:

$$E_{nm}^{H}\ T_{\text{TSAR}}\ E_{nm} \le \text{TSAR}_{\text{max}} \tag{17}$$

where T_{TSAR} represents a Hermitian matrix that determines the radiative balance between the beam produced by the focused antenna system and the peripheral tissues of the target area. This matrix provides the principle of isolation for tissues in non-target areas. As for TSAR_{max}, it expresses the maximum level of TSAR that is used globally for medical safety based on certain tissue weights, for example, 15 g. Then, the final resulting TSAR is:

$$\text{TSAR} = E_{nm,\,final}^{H} T_{\text{TSAR}} E_{nm,\,final} \le \text{TSAR}_{\text{max}} \tag{18}$$

To ensure the therapeutic durability of the resulting beam pattern, the minimum radiation was directed to the target area. Therefore, the main objective is to match the resulting pattern to the shape of diseased tissue. Here, the importance of generating a sufficient electromagnetic field for the target area must

be considered, given the presence of inactive elements owing to the application of the sparse technique. Therefore, a specific targeting constraint is imposed on the diseased tissues to ensure that sufficient, directed, and non-dispersed electromagnetic energy is delivered, as follows:

$$|\mathbb{F}(\theta_o, \phi_o)| \geq P_{\min} \tag{19}$$

where (θ_o, ϕ_o) represents the radiation coordinates directed towards the area to be treated with radiation, and $P_{\min}$ represents the minimum of the electromagnetic field. The proposed synthesis approach works to make the method of forming the therapeutic pattern non-convex and high-dimensional waveforms consisting of a series of sub-processors that are constructed computationally and mathematically, thus ensuring the convergence of results for each improvement stage and producing a high improvement efficiency. This is represented in the first and third parts of Eq. (12), i.e.,

$$\min_{E_{nm}} \| |\mathbb{F}(\theta, \phi)| - I \|_2^2 + \alpha_2 \|E_{nm}\|_2^2 \tag{20}$$

Therefore, the excitation E_{nm} is calculated periodically with each execution of the algorithm as follows:

$$E_{nm_o} = \left(P^H P + \alpha_2 \Upsilon\right)^{-1} P^H I \tag{21}$$

where Υ represents a unity identity matrix. This stage (i.e., Eqs. (17) and (18)) formulated a beam pattern that is exactly similar to the organ to be treated with radiation, in the form of a perfectly convex quadratic mathematical model, which ensures convergence and reaches the optimal solution. The second stage introduces the efficient sparsing property by repeatedly applying the zero-norm principle. Therefore, the positions of the active elements can be continuously updated with each execution of the algorithm, depending on the shape of the diseased organ, as follows:

$$\alpha_n^{(i)} = \frac{1}{\left|E_{nm}^{(i)}\right| + \Delta} \tag{22}$$

Therefore, the final optimization problem is:

$$\min_{E_{nm}} \| |\mathbb{F}(\theta, \phi)| - I \|_2^2 + \sum\nolimits_n \sum\nolimits_m \alpha_{nm}^{(i)} |E_{nm}|^2 \tag{23}$$

$$E_{nm_o}^{(i+1)} = \left(P^H P + \alpha_2 \Upsilon^{(i)}\right)^{-1} P^H I \tag{24}$$

The clinical efficacy of creating a therapeutic electromagnetic beam pattern depends on the degree of conformity between the pattern and the target area shape. This is assessed by measuring the signal-to-noise ratio (SNR_{peak}) parameter as follows:

$$\mathrm{SNR}_{peak} = 10 \log_{10} \left(\frac{\max(|\mathbb{F}(\theta, \phi)|_{fidelity}^{final})^2}{\frac{1}{\phi_R} \int_{\phi_R} \left| |\mathbb{F}(\theta, \phi)| - |\mathbb{F}(\theta, \phi)|_{fidelity}^{final} \right|^2 d\phi_R} \right) \tag{25}$$

Finally, the final sparsity ratio (FSR), beam pattern matching error (BPME), and convergence speed (CS) resulting from the proposed optimization algorithm are determined by measuring the following models:

$$\mathrm{FSR} = \frac{\left\|E_{nm}^{final}\right\|_0}{NM} \tag{26}$$

$$\mathrm{BPME} = \frac{\|\mathbb{F}(\theta, \phi)_{resulted} - \mathbb{F}(\theta, \phi)_{desired}\|_2^2}{\|\mathbb{F}(\theta, \phi)_{desired}\|_2^2} \tag{27}$$

$$\mathrm{CS} = \frac{convergence\ iteration}{total\ number\ of\ iteration} \times 100\% \tag{28}$$

The proposed mathematical model scenario for building a therapeutic radiation system is illustrated in Figure 1.

4. SIMULATION RESULTS

Several mathematical coordinates, changes in the electric field, and software tools must be prepared before conducting simulated measurements to synthesize therapeutic radiation patterns.

4.1. Forming the Dimensions of True Bio Radiation

Typically, in an antenna array, beam patterns are synthesized in space within the spatial coordinate dimensions of the frequency domain (uv). However, in medical applications, these dimensions are considered incompatible with the precise dimensions of the organs. Therefore, an adaptive conversion procedure must be performed in the applied electromagnetic field to make it suitable for biophysical medical applications. This produces a pattern that can be physically explained in terms of the biological analysis of the tissues. This procedure offers several advantages from medical and engineering perspectives, including clinical treatment accuracy and design soundness. To accomplish this, the cosine coordinates defined in Eq. (2) (i.e., $\sin\theta\cos\phi$, $\sin\theta\sin\phi$) must be transformed because they do not represent the directions of the physical biomedical pattern, despite being suitable for the array coordinates. The conversion process is tailored to the area of the generated main beam and is similar to the diseased target area by calculating the inverse triangular conversion of this area. Another problem that must be considered is the depth of propagation and penetration of electromagnetic waves within the targeted tissues. This problem was solved by converting the area of the directed beam region into spatial coordinates based on the wave propagation phenomenon. This procedure provides accurate peripheral measurements of the generated and directed radiation pattern in the human body, as well as its penetration into tissues. Consequently, it offers a direct measurement of the electromagnetic energy directed to the target area and not consumed by other areas. From a design perspective, the operating frequency is used to construct the true dimensions of a therapeutic pattern. By selecting the appropriate frequency to target a specific organ in the human body, the frequency wavelength is fixed, which determines the distance between the antennas in the array and the size of the array aperture. This allows for the verification of the antenna system's structure and practical feasibility, ensuring patient safety and clinical application. In addition, choosing the appropriate frequency provides knowledge of the depth of

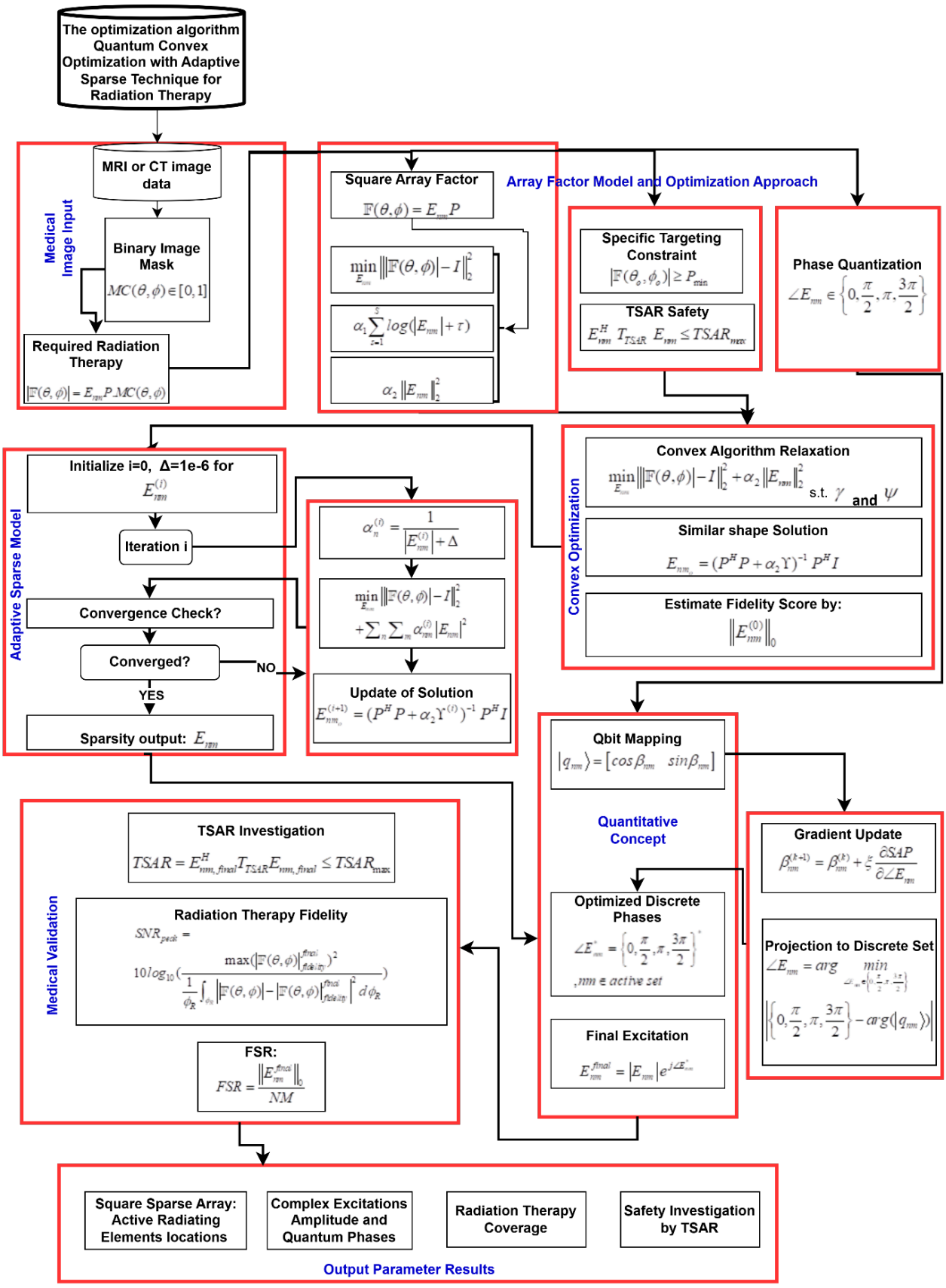

FIGURE 1. The proposed optimization procedures.

TABLE 2. Frequency range allocated for medical treatment.

Targeted Organ	Resonant Frequency (GHz)
Superficial	5.8
Breast	2.45
Liver	0.915–2.4
Kidney	0.915–2.4
Brain	0.915

penetration of the electromagnetic field into biological tissues and the rate of energy absorption. Table 2 presents the range of frequencies allocated for medical treatment. Finally, in the preparation stage, the beam pattern directed at a specific organ should be measured in true anatomical dimensions (millimeters or centimeters). This is achieved by importing medical images from various medical imaging devices, such as MRI and CT, after the tumor has been accurately located and its sides identified to build a suitable spatial area to generate a compatible beam pattern. The energy of the pattern is concentrated in its main beam to be directed at the tumor for removal, while reducing energy in other areas by significantly reducing the sidelobes, with the possibility of generating deep null zones to protect healthy tissues near the tumor.

4.2. Simulation Measurements

To demonstrate the effectiveness of the proposed approach in synthesizing specialized therapeutic beam patterns for human tissues, several simulated scenarios were presented. A synthesis method based on improving the amplitude and phase excitation of elements in a square array aperture consisting of 20×20 elements with equal dimensions equal to 0.4λ, with the possibility of decreasing or increasing the number of elements. The optimization task was assigned to the QCA to build an irregular beam pattern that mimics the irregular shape of diseased tissues with the ability to generate high spatial selectivity. A sparse technique was added to the optimization process to reduce systemic and computational complexity. The proposed approach has the design capability to run all the frequencies shown in Table 2. That is, the simulated synthesis process in MATLAB can run at any vital application frequency and therefore can be built into the Computer Simulation Technology (CST) program in the future to develop this research practically. Several synthesis scenarios, ranging from building a pattern that mimics the entire shape of the human organ to creating a pattern limited to the diseased area within the organ (a tumor, for example), were presented and are shown in the following sections. In all simulated tests, a set of illustrations such as a binary image of the target area, a contour drawing, a three-dimensional polar drawing, a TSAR, and a distribution of sparse elements is displayed. In all presented experiments, the 2D TSAR calculation was performed according to the specifications shown in Table 3, in accordance with the IEEEC95.1 standard (this standard defines the medical safety limits for protecting humans from the effects of exposure to electromagnetic fields within the frequencies of 3 KHz to 300 GHz). In all investigations, a study tissue was proposed that matches human tissue in terms of electrical and physical properties at 2.4 GHz. The physical parameters ρ and σ values of 1050 kg/m^3 and 1.4 S/m, respectively, were considered based on dielectric properties, with the radiation exposure area defined in units of volume, for example, 10^{-3} m^3. The radiated energy of the sparse array was calibrated at 1 W and directed to the target area. This energy was then spatially distributed to the tissues of the target organ according to the square of the calibrated value of the optimized array factor. It is important to note that the presented TSAR results in this study are computational, mathematical, and simulated for investigative purposes. Actual TSAR measurements can be performed on anatomically detailed human tissues using electromagnetic simulations based on precise pixels, and this is what we will investigate in future research.

TABLE 3. The IEEEC95.1 standard.

Parameter	Value	Unit
Free-space wavelength	0.122	m
Electrical conductivity σ	1.4	S/m
Mass density ρ	1050	kg/m³
Electric field scaling factor	100	V/m
SAR safety limit	2.0	W/kg
Tissue model	Homogeneous	—
Exposure regime	Continuous-wave	—

Test 1: Full organ pattern shaping (Liver organ, for example)

In this section, to construct a radiographic pattern that resembles the organ, taking into account its irregular structure and constituent tissues, the tomographic image taken from the medical imaging device is considered. The image of the organ, with all its details, is isolated into an image consisting of only two colors, black and white, through the use of a digital image processing technique. It is important to take into account that the processed image is high-resolution in two colors only. The white color represents the targeted tissue area, and the black color represents the non-targeted area. After preparing the required medical image, it is entered into the proposed antenna system in order to synthesize the required therapeutic beam pattern. Then, the composed beam is directed to the target area in the human body. Figure 2 shows the results of the computer simulation. Figure 2(a) represents the binary image extracted from the medical imaging device and prepared for entry into the proposed medical beam system. Figure 2(b) shows the contour representation of the pattern resulting from the optimization algorithm. Contour representation provides a structural illustration of the treatment pattern along with a demonstration of the distribution gradients of radiation power. It also provides a clear, debatable view of focusing the treatment footprint in the targeted area while effectively protecting healthy surrounding tissues. Figure 2(c) illustrates the three-dimensional polar representation of the organ. It can be observed from this figure that the directed main area beam has taken on a flat, flexible shape without any rippling in its surface area, while possessing a sharp spatial depression. Synthesizing such patterns is not easy, and this demonstrates the robustness of the proposed approach to high-level control of electromagnetic wave propagation. Such

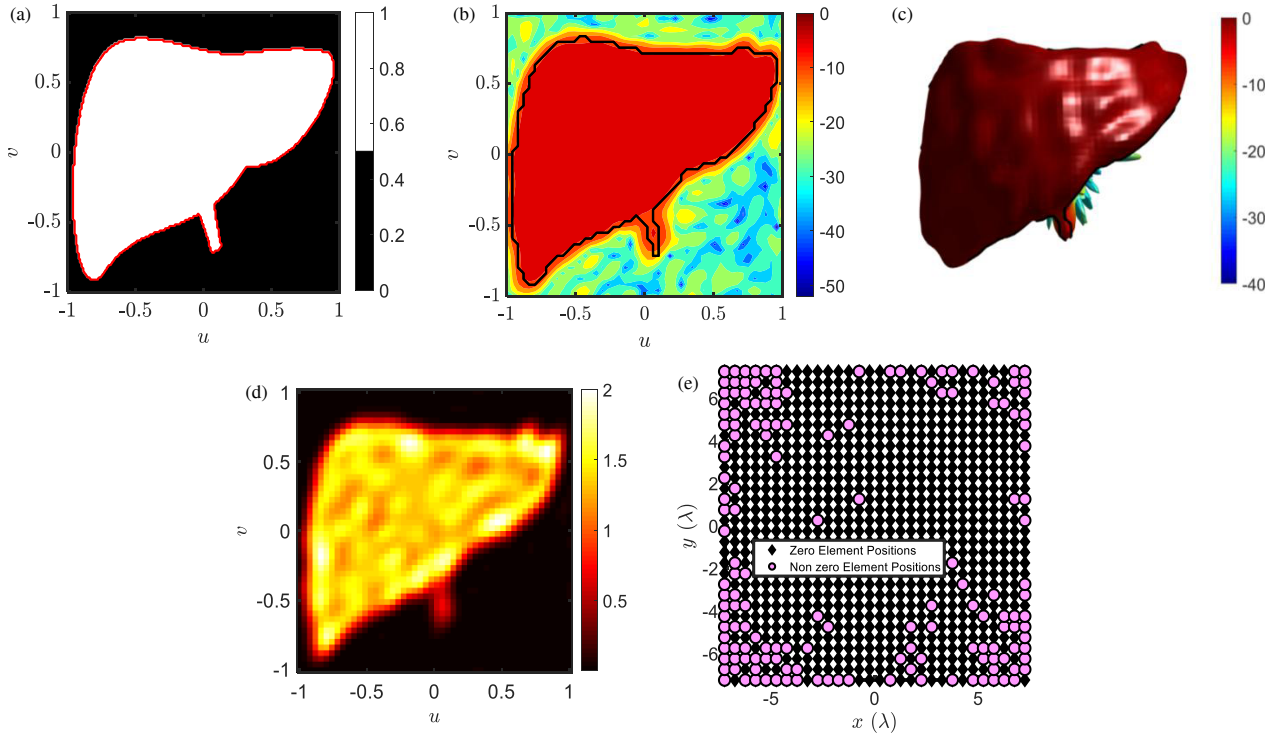

FIGURE 2. The results of test 1. (a) The binary image, (b) contour radiation plot, (c) polar radiation plot, (d) TSAR measurement, and (e) sparse elements distribution.

results are important in medical applications, providing high protection for the human body from exposure to high electromagnetic radiation. The isolation of the electromagnetic field was achieved by reducing the level of the sidelobes to -30 dB or less. Figure 2(d) represents the antenna aperture designed as a square array showing the locations of the active elements involved in the synthesis process. It can be observed from this figure that a large group of radiating elements, amounting to 70%, were turned off, while the active elements amounted to 30%. Dealing with a small number of active elements in array synthesis gives many advantages, including reducing systemic and computational complexity, as well as reducing the time spent on displaying medical results. One of the most important measurements in radiotherapy is determining the amount of energy absorbed by tissues.

This is done using the TSAR meter, which accurately provides the specific absorption rate of electromagnetic radiation to the target area and limits the effectiveness of radiation absorption in healthy tissues. Figure 2(e) illustrates the relationship between the amount of energy absorbed and the spatial distribution of TSAR. This figure shows that the amount of radiation penetrating the tissues in the target area is greater than in other areas, which confirms our claim. It can be observed from this figure that a boundary mask has been formed for the coverage area, and the radiation direction is clearly restricted to the target area, giving a higher concentration of the TSAR value inside the intended tissue area and a lower concentration outside it. These results confirm the effectiveness of targeted radiation sizing in the targeted area to achieve concentrated energy deposition, fulfilling a key requirement in therapeutic radiation applications. Based on the criteria shown in Table 2, the value of TSAR was made to be less than the internationally accepted threshold limit (TSAR $\leq$ 2 W/kg), which demonstrates the effectiveness of the antenna array design in medical applications.

Test 2: Pattern shaping for a part of an organ

In many cases of illness, a part of the human body is affected by a disease that requires effective and precise treatment. For radiation therapies, a difficult challenge arises in allocating a suitable electromagnetic radiation beam that requires protecting some of the shared tissues between the diseased and undiseased areas in the same organ when the beam is applied. Therefore, to clarify this problem, a liver organ affected by a localized partial tumor in a specific area is considered. Figure 3 illustrates the results of this problem. Figure 3(a) shows the targeted area within the organ after conversion to a binary image. Figure 3(b) shows the contour representation of the radiographic measurement for this issue. It can be observed from this diagram that the boundaries of an irregular, flat covering radiation have been drawn, taking the shape of the swollen, diseased area, while accurately showing the isolation of healthy tissues in the same organ. This is the desired outcome. This property provides high therapeutic flexibility in the process of adaptively combining different forms of radiation, thus enabling the use of the same array system in treating different diseases in different locations. Figure 3(c) illustrates the directed polarized view from the medical radiation device to the target area with high accuracy by forming a homogeneous three-dimensional beam pattern without oscillations. Figure 2(d) shows the locations of the active elements, and their number is considered large compared to the first case. The amount of processed electromagnetic ra-

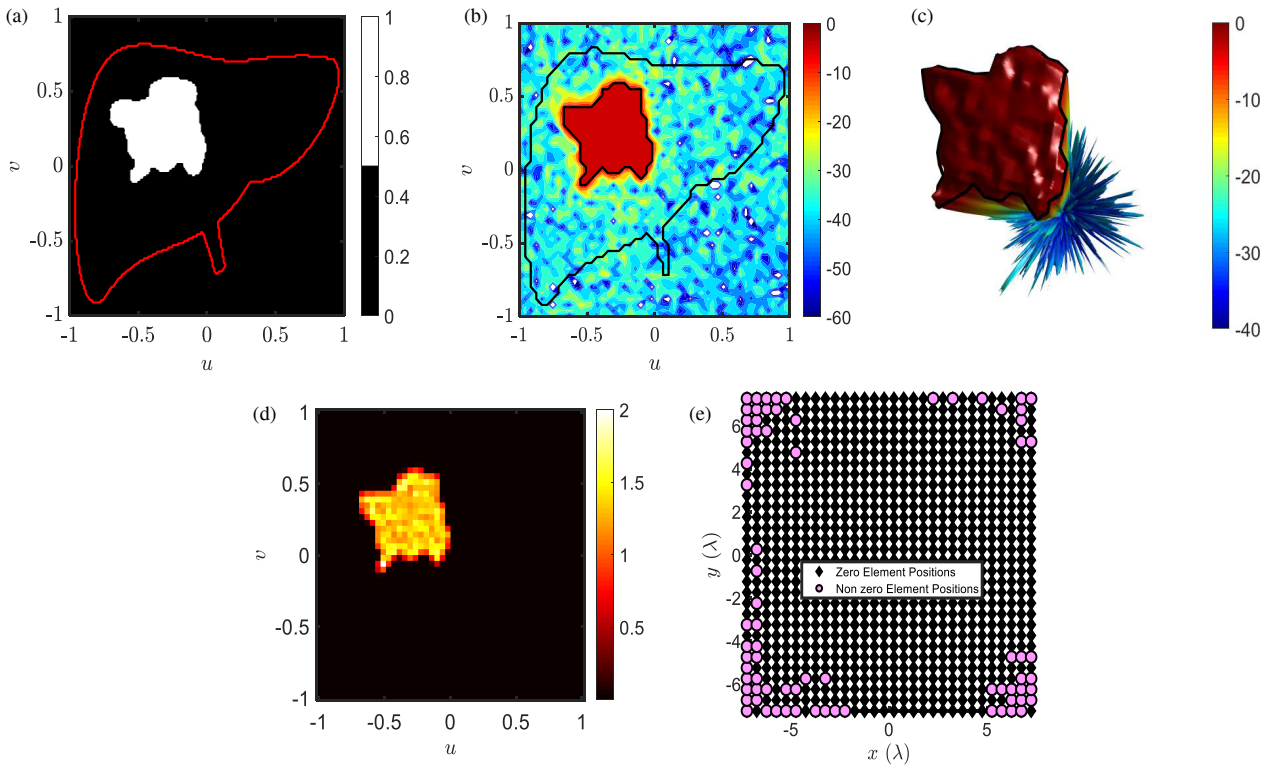

FIGURE 3. The results of test 2. (a) The binary image, (b) contour radiation plot, (c) polar radiation plot, (d) TSAR measurement, and (e) sparse elements distribution.

TABLE 4. Parameter results comparison between the proposed method and some references.

Ref.	Number of elements	Excitation type	Algorithm type	PSLL dB	Irregular pattern shaping	pattern matching error	FSR %	convergence speed
[14] Figure 6	400	Complex	Compressed sensing	−13.6	No	10^{-3}	40	Fast
[15]	800	Complex	Bayesian Compressed Sensing	−20	No	10^{-3}	45	Very fast
[16]	400	Complex	Bayesian Compressed Sensing	−35	No	10^{-2}	13–75	Very fast
[17]	32	Position-only	IWO/WDO	−23.5	No	Indirect with respect to SLL and null steering	55	Very fast
This work	900	complex	QCA	-30	yes	10^{-2}	18.5	Fast
			QCA	−30	yes	10^{-2}	15.5	Fast
			QCA	−30	yes	10^{-2}	69.5	Fast

diation penetrating the target area can be seen in Figure 3(e). This figure shows that peripheral tissues are less permeable to this radiation.

Test 3: Pattern shaping for two or more parts of an organ

In this section, the construction of a therapeutic beam pattern that simulates more than one diseased area within a single organ is presented. Figure 4 shows a set of special cases. The challenge in this case is the proximity of the diseased tissues to each other, which creates narrow areas of healthy tissue very close to the target tissues. Therefore, the proposed approach considers this, as illustrated in Figure 4(b). Such referrals require the participation of a relatively large number of radiating elements in the synthesis.

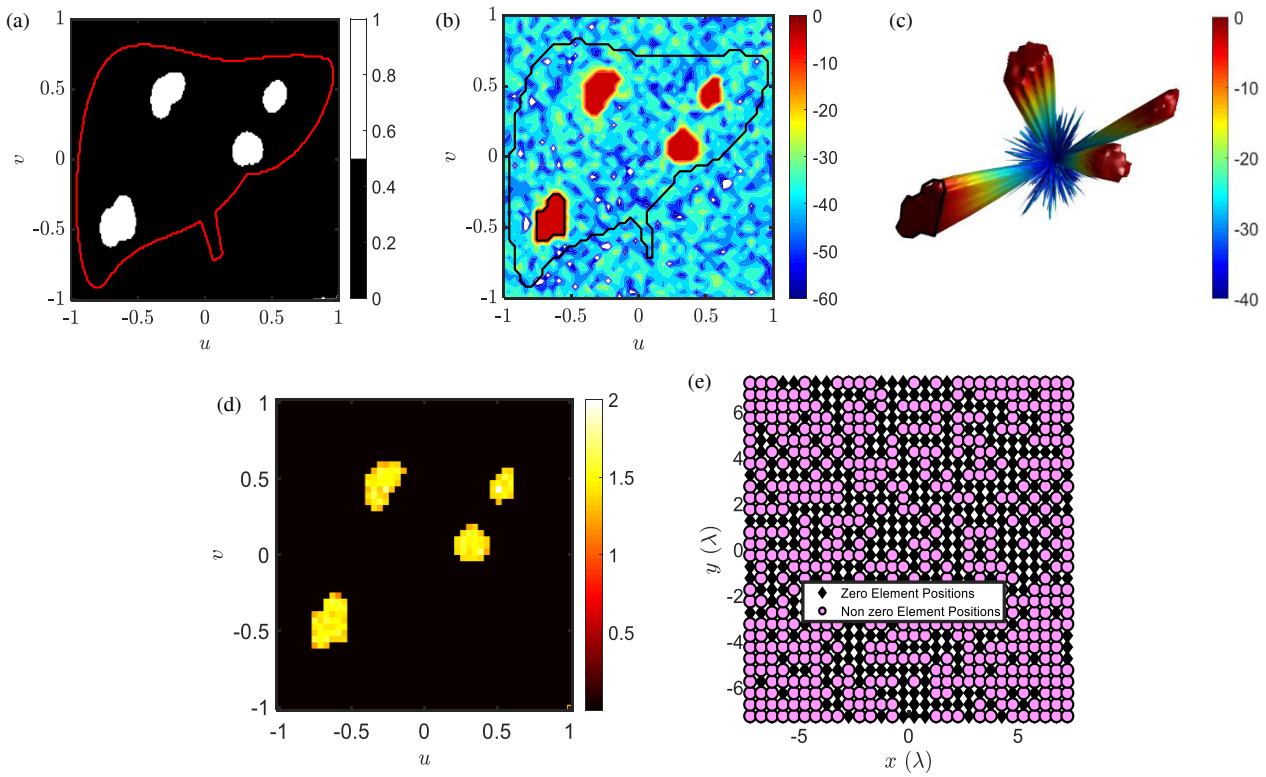

FIGURE 4. The results of test 3. (a) The binary image, (b) contour radiation plot, (c) polar radiation plot, (d) TSAR measurement, and (e) sparse elements distribution.

To demonstrate the robustness of the proposed method, a set of comparisons, shown in Table 4, was conducted with the results of previous research under the following parameters: number of elements, excitation type, algorithm, peak sidelobe level (PSLL), irregular pattern shaping, pattern matching error, FSR, and convergence speed. Despite employing various very rapid optimization methods in the research listed in Table 4, these references lacked the ability to form irregular patterns mimicking different shapes. The proposed method achieved high-performance electromagnetic specifications in terms of forming a beam pattern that mimics a high-precision human organ with a significant reduction in PSLL reaching more than -30 dB, in addition to reducing the number of active elements responsible for radiation. Other research has not been able to meet these requirements for effective medical applications.

5. CONCLUSION

The results demonstrate the effectiveness of the proposed approach in synthesizing therapeutic radiation patterns generated by an antenna array system. The proposed scenario relies on a hybrid optimization algorithm that integrates several optimization techniques, exploits the concept of quantum computing and convex theory, and finally, applies the theory of mitigating sparsity. The radiation system employed demonstrated its ability to generate diverse and irregular radiation patterns based on binary images obtained from medical imaging devices, relying on a small number of active radiating elements only. Based on the results obtained from computational measurements, this study presents a method for directing electromagnetic radiation patterns capable of isolating both the target and non-target regions (by maintaining the sidelobes at -30 dB or below). This was achieved through precise measurements, such as the contour, TSAR, and polar plotting of the pattern. Finally, the results of the radiation system can be verified through physical design using CST software to evaluate the effectiveness of the proposed method in biomedical applications.

REFERENCES

[1] Rosen, A., M. A. Stuchly, and A. V. Vorst, "Applications of RF/microwaves in medicine," *IEEE Transactions on Microwave Theory and Techniques*, Vol. 50, No. 3, 963–974, 2002.

[2] Lantis II, J. C., K. L. Carr, R. Grabowy, R. J. Connolly, and S. D. Schwaitzberg, "Microwave applications in clinical medicine," *Surgical Endoscopy*, Vol. 12, No. 2, 170–176, 1998.

[3] Dewhirst, M. W., B. L. Viglianti, M. Lora-Michiels, M. Hanson, and P. J. Hoopes, "Basic principles of thermal dosimetry and thermal thresholds for tissue damage from hyperthermia," *International Journal of Hyperthermia*, Vol. 19, No. 3, 267–294, 2003.

[4] Kampinga, H. H., "Cell biological effects of hyperthermia alone or combined with radiation or drugs: A short introduction to newcomers in the field," *International Journal of Hyperthermia*, Vol. 22, No. 3, 191–196, 2006.

[5] Lagendijk, J. J. W., "Hyperthermia treatment planning," *Physics in Medicine & Biology*, Vol. 45, No. 5, R61–R76, 2000.

[6] Fenn, A. J., *Adaptive Phased Array Thermotherapy for Cancer*, Artech House, 2008.

[7] Nikolova, N. K., "Microwave imaging for breast cancer," *IEEE Microwave Magazine*, Vol. 12, No. 7, 78–94, 2011.

[8] Brown, A. D., *Electronically Scanned Arrays MATLAB® Modeling and Simulation*, CRC Press, 2017.

[9] Stang, J., M. Haynes, P. Carson, and M. Moghaddam, "A preclinical system prototype for focused microwave thermal therapy of the breast," *IEEE Transactions on Biomedical Engineering*, Vol. 59, No. 9, 2431–2438, 2012.

[10] Nguyen, P. T., A. Abbosh, and S. Crozier, "Three-dimensional microwave hyperthermia for breast cancer treatment in a realistic environment using particle swarm optimization," *IEEE Transactions on Biomedical Engineering*, Vol. 64, No. 6, 1335–1344, 2017.

[11] Abdulqader, A. J. and J. R. Mohammed, "New improved Sierpinski carpet structures based thinned planar array to synthesize low sidelobes radiation pattern," in *2023 International Conference on Radar, Antenna, Microwave, Electronics, and Telecommunications (ICRAMET)*, 178–183, Bandung, Indonesia, 2023.

[12] Abdulqader, A. J., "Different 2D and 3D mask constraints synthesis for large array pattern shaping," *International Journal of Microwave and Wireless Technologies*, Vol. 16, No. 4, 579–587, 2024.

[13] Abdulqader, A. J., A. N. Mahmood, and Y. E. M. Ali, "A multi-objective array pattern optimization via thinning approach," *Progress In Electromagnetics Research C*, Vol. 127, 251–261, 2022.

[14] Mohammed, J. R., R. H. Thaher, and A. J. Abdulqader, "Linear and planar array pattern nulling via compressed sensing," *Journal of Telecommunications and Information Technology*, Vol. 85, No. 3, 50–55, Sep. 2021.

[15] Oliveri, G., M. Carlin, and A. Massa, "Complex-weight sparse linear array synthesis by Bayesian compressive sampling," *IEEE Transactions on Antennas and Propagation*, Vol. 60, No. 5, 2309–2326, 2012.

[16] Viani, F., G. Oliveri, and A. Massa, "Compressive sensing pattern matching techniques for synthesizing planar sparse arrays," *IEEE Transactions on Antennas and Propagation*, Vol. 61, No. 9, 4577–4587, 2013.

[17] Mahto, S. K. and A. Choubey, "A novel hybrid IWO/WDO algorithm for interference minimization of uniformly excited linear sparse array by position-only control," *IEEE Antennas and Wireless Propagation Letters*, Vol. 15, 250–254, 2016.